Resource Management for Sum-rate Maximization in SCMA-Assisted UAV System

Saumya Chaturvedi, Vivek Ashok Bohara, Zilong Liu, Anand Srivastava, Pei Xiao

***Abstract*—This work presents a resource management framework for optimizing the sum-rate in a sparse code multiple access (SCMA)-assisted UAV downlink system. We formulate two optimization problems for maximizing the overall sum-rate: the first problem addresses UAV 3D deployment and trajectory optimization with energy constraints, while the second focuses on optimizing SCMA subcarrier and power allocation optimization, subject to factor graph matrix (FGM) constraints and a minimum user data rate. Since the optimization problems are non-convex, the complexity of finding the global optimal solutions is prohibitive. We propose a gradient ascent-based iterative algorithm to compute the optimal UAV 3D deployment and trajectory. Further, an effective channel state information-based algorithm is proposed for FGM assignment, followed by a Lagrange dual decomposition method to solve the power allocation problem efficiently. Our research findings demonstrate that the optimization of the UAV trajectory gives improved sum-rate within the specified energy budget. Further, employing CSI-based multiple subcarrier allocation and strategic power allocation can significantly improve system performance compared to the benchmark schemes.**

***Index Terms*—Resource Management, 3D trajectory design, Probabilistic LoS channel, Sparse Code Multiple Access (SCMA), Unmanned Aerial Vehicles (UAV) communications.**

I. Introduction

With the wide commercialization of the fifth generation (5G) mobile communication systems, the research and development for the sixth generation (6G) of communication systems has started across the world. The target is to provide improved data services for increasingly stringent quality-of-services (QoSs), such as higher capacity and spectrum efficiency, improved robustness, lower latency, and a significantly increased number of communication devices [1]. To realize this vision, it is pressing to further push the limits of wireless system design by studying various disruptive wireless technologies [2].

Recently, unmanned aerial vehicles (UAVs) have found wide applications in a number of use cases, such as forest fire detection, emergency search and rescue, traffic controls, etc [3]. UAVs will also play an essential role in the next-generation wireless communication systems [4]. UAV-assisted networks offer various advantages compared to the conventional communication systems that heavily rely on terrestrial base stations (BSs). The agile mobility and maneuvering prowess of UAVs empower them to establish direct line-of-sight (LoS) connections with a majority of communication devices [5]. Compared to terrestrial BSs, UAVs can be employed in a variety of environments with difficult geographical conditions. This can be made by designating a UAV as a mobile BS for rapid deployment to the target areas (e.g., hotspots or remote villages/forests) for real-time on-demand coverage.

For UAVs to efficiently communicate with a massive number of devices/sensors on the ground, there is a acute need to develop highly spectrum-efficient multiple access techniques. Conventional communication systems generally use orthogonal multiple access (OMA) schemes in which each resource element (RE) (e.g., frequency, time, or code) is utilized by a single user. However, it is conceivable that OMA may not meet the rigorous demands imposed by future wireless applications. In view of this, non-orthogonal multiple access (NOMA) techniques have been extensively studied owing to their advantages of providing more concurrent communication links, reduced access latency, and higher spectral efficiency [6], [7].

In NOMA, the fundamental concept involves efficiently catering to a large number of users by employing non-orthogonal overloading of REs. NOMA is primarily categorized in two domains: power-domain NOMA (PD-NOMA) and code-domain NOMA (CD-NOMA). In PD-NOMA, users are allocated distinct power levels contingent upon their respective channel conditions [8]. In CD-NOMA, individual users are assigned a distinct CB or signature sequence. Sparse code multiple access (SCMA) is one of the prominent techniques proposed among many CD-NOMA schemes [9]. In SCMA, the bits corresponding to each user are directly mapped to a codeword which is extracted from its associated codebook (CB) [9]. Thanks to its coding gain and constellation shaping gain, there is improvement in sum-rate and bit error rate (BER) [10]–[12]. Further, several low-complexity detection methods have been proposed for SCMA systems, both in static [13] and mobile environments [14]–[16]. With the increasing demand for higher capacity and massive connectivity in future wireless applications, there is a strong interest in investigating the integration of SCMA with UAV to explore higher performance gains.

The structure of the paper is outlined as follows. Section II delves into a discussion of the related works. Section III presents the UAV-SCMA system model and the formulated

Saumya Chaturvedi, Vivek Ashok Bohara, and Anand Srivastava are with Indraprastha Institute of Information Technology (IIIT-Delhi), Delhi, New Delhi, 110020, India (e-mail: {saumyac, vivek.b, anand}@iiitd.ac.in). Zilong Liu is with the School of Computer Science and Electronics Engineering, University of Essex, Colchester CO4 3SQ, U.K. (e-mail: zilong.liu@essex.ac.uk). Pei Xiao is with Institute of Communication Systems (ICS), 5GIC & 6GIC, University of Surrey, UK (e-mail: p.xiao@surrey.ac.uk)

optimization problem. Section IV discusses the proposed solution. The results are presented and discussed in Section V. Subsequently, the conclusive remarks are described in Section VI.

II. Related Works and Contributions

Several research works based on the integration of NOMA with UAV systems are documented in the literature [17]–[32]. In [18], N. Zhao *et al.* worked on the security aspect of NOMA-UAV networks and proposed two secure transmission schemes by beamforming optimization and power allocation, respectively. Sun *et al.* [19] investigated a downlink cyclical NOMA-based UAV network and optimized UAV trajectory and multi-user communication scheduling to maximize the minimum user rate. In [20], the UAV 2D placement, admission control, and NOMA power allocation were optimized in order to maximize the number of users with a satisfied QoS experience. The uplink NOMA random access (RA) was studied in [21], in which the maximum stable throughput was characterized in terms of the UAV's altitude and beamwidth. P. Qin *et al.* utilized UAVs for access and high altitude platform stations (HAPSs) for data backhaul to establish the air-ground integrated network (AGIN), and achieve uninterrupted coverage for remote Internet of Things (IoT) devices [22].

NOMA allow us to fully use the potential of UAV networks, even for single antenna ground users with single-antenna UAV-BS. Within the context of *NOMA-assisted UAV systems*, several works investigate joint optimization of various optimization variables such as UAVs placement [18], [23], [24], UAVs trajectories [19], [22], [25], [26], [29]–[31], power allocation [18], [20], [22]–[25], [29], [30], [32] and subchannel allocation [22], [31]. They have worked to improve various performance objectives, including capacity [21], [23], [24], [26], [30], maximize the minimum user rate [25], [32], energy efficiency [22], [29], uplink energy minimization [31], and secrecy [18].

Comparatively fewer studies have been done on the resource management aspects of SCMA. In general, the BS allocates uniform power to all users without considering channel state information (CSI). The issue of resource allocation for SCMA was addressed in [33]–[37]. The fundamental tradeoff between rate and energy was investigated in a downlink SCMA system for the predesigned CBs [33]. The authors in [34] optimized both CB and power allocation within the downlink device-to-device (D2D) enabled cellular network with the objective of maximizing the overall system data rate. A three-level power allocation model was proposed in [46] to maximize the capacity. M. Cheraghy *et al.* worked on multi-objective resource allocation to maximize the average sum-rate in an uplink SCMA system [35]. In [36], CB selection and bandwidth allocation were optimized to maximize the sum rate in an uplink SCMA based vehicle-to-everything (V2X) networks. In [37], resource allocation was done for a downlink intelligent reflecting surface (IRS)-aided SCMA system for sum-rate maximization. The resource management in a SCMA-aided UAV network has not yet been explored, to the best of our knowledge.

A. Motivations and Contributions

It is noticeable from the above-mentioned literature that the NOMA-assisted UAV systems are more efficient in providing improved QoSs. However, most of these works focused on integrating PD-NOMA with the UAV systems. The performance of PD-NOMA in UAV communications, however, may not be guaranteed due to the following reasons: 1) A perfect successive interference cancellation (SIC) technique is often used at the receiver side, which may not be possible in complex wireless channels; 2) SIC depends on the accurate CSI in order to determine the right decoding order, but this may be difficult in view of the mobile UAVs; 3) The user pairing of PD-NOMA could consume a significant amount of system resources, especially in a dynamic moving environment.

In contrast to the existing works, we study the integration of SCMA with UAV systems. The PD-NOMA provides performance gains over OMA schemes when the user pair has distinctive channel conditions [38]. Thus, PD-NOMA requires additional constraints of user pairing and reordering in the optimization problem. However, SCMA does not need such stringent constraints. In SCMA, each user is active on more than one RE, and users are divided into several groups depending on the locations. The SCMA system is different from any other communication system. SCMA enjoys a constellation shaping gain because of the use of multi-dimensional CBs, and thus, it outperforms other NOMA techniques in terms of the spectral efficiency [9], [10]. Also, SCMA outperforms the current LTE and PD-NOMA RA procedure relating to access delay and access success probability [12]. As a contemporary variant of code division multiple access, SCMA overcomes the aforementioned difficulties/challenges of PD-NOMA along with improved error rate performance [11].

This paper considers a SCMA-assisted UAV communication scenario, in which the aim is to utilize the available resources efficiently, and maximize the system data rate. The overall energy consumption of UAVs is primarily categorized into two components: energy utilized for communication and propulsion energy. In this work, the following three types of resources are studied: (1) propulsion energy allotted to the UAV to reach the hovering point, (2) transmit power at UAV for communication, and (3) available spectral resources at the UAV. Towards this direction, we first focus on the optimization of UAV 3D placement by maximizing the system sum-rate. Next, we compute an optimal UAV 3D trajectory from the given initial position to the final deployment location considering the available on-board energy. After arriving at the hovering point, spectral resources and transmit power at the UAV are allocated to each user to maximize the system sum-rate. This framework is applicable to many practical scenarios, such as providing data service to the first responders in a disaster-affected areas or offloading data traffic in a crowded area. The main contributions of this work are:

- First, we formulate an optimization problem to maxi-

TABLE I
COMPARISON OF THE PROPOSED WORK WITH OTHER WORKS ON NOMA-ENABLED UAV SYSTEM

Reference	UAV Deployment	UAV Trajectory	Power Allocation	Subchannel Allocation	Problem Formulation
[18]	UAV 2D position	✗	✓	✗	Security enhancement via power allocation and beamforming
[19]	✗	2D trajectory	✗	✗	Maximize the minimum rate in cyclical-NOMA based UAV-network via optimizing user scheduling and trajectory with LoS channel model.
[20]	UAV 2D position	✗	✓	✗	Maximize the number of users with satisfied QoS via admission control, UAV placement, and power allocation
[22]	✗	2D trajectory	✓	✓	Maximize uplink EE for IoT terminals in AGIN
[23]	UAV altitude	✗	✓	✗	Sum-rate maximization with reducing UAV energy expense.
[24]	UAV 2D position	✗	✓	✗	Sum-rate maximization with LoS dominant path-loss model
[25]	✗	2D trajectory	✓	✗	Maximize the minimum rate for OMA and NOMA modes in LoS dominant path-loss model.
[26]	✗	2D trajectory	✗	✗	Maximize sum-rate via trajectory design, user scheduling and NOMA precoding in LoS dominant model.
[27]	UAV 2D position	✗	✓	✗	Maximize the sum-rate in an uplink NOMA-assisted UAV-assisted data collection (NUDC) system via optimizing the UAV location, sensor grouping, and power allocation.
[28]	✗	2D trajectory	✓	✗	Investigated an uplink UAV-NOMA system for time-efficient data collection by optimizing the UAV trajectory, device scheduling and transmit power.
[29]	✓	✗	✓	✗	Maximize the energy-efficiencyin an uplink NOMA-UAV data collection system
[30]	✗	✓	✓	✗	Mazimize the total throughput using RL algorithm
[31]	✗	2D trajectory	✗	✓	Minimize energy consumption in AGIN via optimizing task offloading, trajectory, and resource assignment
[32]	UAV altitude	✗	✓	✗	Maximize minimum rate via bandwidth allocation and beamwidth optimization.
Proposed work	✓	✓	✓	✓	Sum-rate maximization in a Probabilistic path-loss model

mize the sum-rate for the downlink SCMA-assisted UAV system and optimize the UAV 3D deployment location and UAV trajectory under the available onboard energy.

- Next, we formulate a sum-rate maximization problem, where the multiple subchannel allocation and power allocation matrices are optimized, when UAV reaches the deployment location. The major challenge lies in solving the above problem with low computational complexity subject to the constraints of SCMA factor graph matrix (FGM), UAV transmit power budget, and user required QoS. We show that the formulated optimization problem is a non-convex non-linear integer programming problem.
- We propose an iterative gradient ascent-based algorithm to solve the UAV 3D deployment and trajectory optimization problem for rate maximization. Next, we introduce an efficient factor graph matrix assignment algorithm for allocating subcarriers to each user. Finally, we carry out the power allocation using Lagrange dual decomposition method considering the power budget and minimum user rate constraints.
- Comprehensive simulation results are shown to demonstrate the efficacy of the proposed algorithms for UAV 3D deployment, trajectory design, FGM assignment, and power allocation which improves the sum-rate with respect to the benchmark schemes.

It is noted that optimizing the UAV's deployment position and UAV's trajectory, leads to a substantial improvement in system performance, even without the resource management. Furthermore, the study highlights the significant role of subchannel and power allocation in maximizing the sum-rate of the SCMA-assisted UAV system.

The notations used in the paper are specified as follows: Scalar, vector, and matrix are denoted by x, $\mathbf{x}$, $\mathbf{X}$ respectively. The notations $\mathbb{R}$, $\mathbb{B}$ and $\mathbb{C}$ denote the sets of real, binary, and complex numbers. The expression 'log($\mathbf{x}$)' denotes the natural logarithm of $\mathbf{x}$. A circularly complex Gaussian random variable x with mean μ and variance σ^2 is symbolized as $x \in \mathcal{CN}(\mu, \sigma^2)$. $|x|$ denotes the absolute value of a complex number x, and $\mathbf{I}_K$ is the $K \times K$ identity matrix.

III. System Model and Optimization Problem Formulation

A. System Model

We consider a downlink ($K \times J$) SCMA-assisted UAV system, as shown in Fig. 1. This system comprises a rotary-wing single-antenna UAV functioning as an aerial-BS, providing service to J single-antenna users using K REs. In SCMA, the number of non-orthogonal superposed

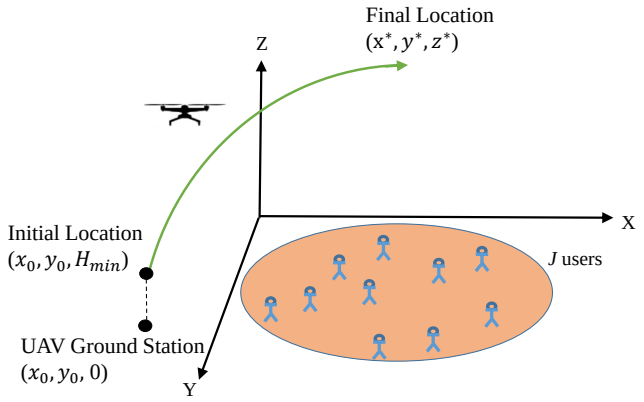

Fig. 1. A plot of the SCMA-assisted UAV system with UAV's 3D trajectory from the predefined initial location to the final deployment location.

codewords can exceed the count of the number of orthogonal REs. This characteristic allows SCMA to accommodate a greater number of users while maintaining the same expanse of resources, thereby enhancing the system capacity.It is assumed that the users are either static or have low mobility, and the location of the jth user is $[x_j, y_j] \in \mathbb{R}^{1\times 2}$. The UAV starts from an initial location $(x_0, y_0, 0)$, moves vertically upwards until it achieves minimum height, and then takes its trajectory toward the final deployment location. The total UAV flight time is divided into M number of time slots of equal duration [4]. The UAV trajectory is denoted as $\mathbf{q}[m] = \{(x[m], y[m], z[m])\}, \forall\ m = 1, \cdots, M$, where $x[m], y[m]$ and $z[m]$ denote the x, y, and z coordinates of the UAV at time slot m.

Let $h_{k,j}$ denotes the channel between the UAV-BS and the jth user at RE k. It is assumed that all the channel vectors are independent complex Gaussian random variables, and all the required channel state information (CSI) is available at the UAV-BS in each time slot. The received signal at RE k is [9]

$$y_k = \sum_{j=1}^{J} h_{k,j} f_{k,j} x_{k,j} + n_k, \tag{1}$$

where $f_{k,j} = 1$ indicates that there is active association between user j and RE k, $x_{k,j}$ indicates the codeword element sent on the kth RE to the jth user, and $n_k \sim \mathcal{CN}(\mathbf{0}, \sigma^2)$ denotes the additive white Gaussian noise (AWGN) at the kth RE. The data received at the jth user on kth RE is interfered from the data of other users communicating over the same RE. Thus, the received signal-to-interference-plus-noise ratio (SINR) of user j at RE k is:

$$\gamma_{k,j} = \frac{|h_{k,j}|^2 p_{k,j}}{\sum\limits_{\substack{i\in S_k \\ i\neq j}} |h^d_{k,i}|^2 p_{k,i}) + \sigma^2}, \tag{2}$$

where S_k represents the set of users communicating over k RE, and $p_{k,j}$ denotes the power allocated to the codeword element $x_{k,j}$.

B. Introduction to SCMA

In SCMA, the binary domain data of multiple users are directly encoded to complex multi-dimensional codewords, with $\bar{M}$ number of codewords in a CB. These codewords are sparse complex vectors with d_v number of non-zero values, $K > d_v$. The improvement in performance achieved by SCMA over other NOMA schemes is contingent upon the meticulous design of sparsely structured CBs. Each user's CB is characterized by its unique sparsity pattern.The problem of CB design in SCMA entails determining the optimal mapping matrix, denoted as $\mathbf{V}^*$, along with the optimal multidimensional constellation, represented by $\mathbf{A}^*$, and can be expressed as

$$\mathbf{V}^*, \mathbf{A}^* = \arg\max_{\mathbf{V},\mathbf{A}} D(S(\mathbf{F}, \mathbf{A}; J, \bar{M}, d_v, K)) \tag{3}$$

where D denotes the design criterion for SCMA system S. The present CB designs are largely sub-optimal, relying on a multi-stage procedure [9]. The CB of user jth of size $K \times \bar{M}$ is given as

$$\text{CB}_j = \mathbf{V}_j \Delta_j \mathbf{A}_{\text{MC}}, \quad \text{for } j = 1, 2, \cdots, J, \tag{4}$$

where $\mathbf{V}_j \in \mathbb{B}^{K\times d_v}$ represents the mapping matrix, Δ_j represents the constellation operator for the jth user and $\mathbf{A}_{\text{MC}}$ represents the multi-dimensional mother constellation. The selection of the mapping matrix is done in a manner that each user is active over a specific set of REs only. Each column of the FGM is $\mathbf{f}_j = \text{diag}(\mathbf{V}_j \mathbf{V}_j^T)$. After determining the mapping matrices, the subsequent step involves designing the mother constellation $\mathbf{A}_{\text{MC}}$ and the constellation operator Δ_j. For designing the multi-dimensional constellations, it is imperative to consider various key performance indicators (KPIs). These include metrics such as Euclidean distance, Euclidean kissing number, Product distance, Product kissing number, and the diversity order of the multi-dimensional constellation points. The aim is to design a multi-dimensional constellation with power variation and dimensional dependency among the constellations [9].

SCMA is primarily characterized by its sparse CBs, and the association between REs and users in SCMA can be depicted through a bipartite factor graph. Here, we have considered a regular factor graph, wherein each user node (UN) is connected to d_v neighboring resource nodes (RNs), and each RN is linked to d_f neighboring UNs. Fig. 2 illustrates the user-RE association through a factor graph, where circles represent UNs and boxes represent RNs. Here, the first RN is linked to the second, third, and fifth UNs, indicating that the data of the second, third, and fifth users is transmitted through the first RE. The association between UNs and RNs can also be expresses through a FGM, $\mathbf{F}$. Consider the FGM denoted by $\mathbf{F} \in \mathbb{B}^{K\times J}$ with each element represented by $f_{k,j}$. The FGM corresponding to the factor

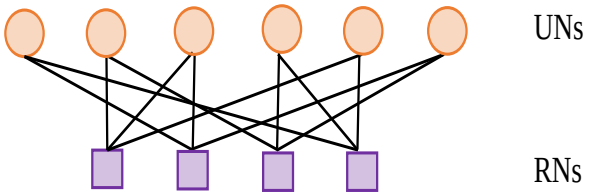

Fig. 2. A regular SCMA factor graph with $d_f = 3$ and $d_v = 2$.

graph shown in Fig. 2 is

$$\mathbf{F}_{4\times 6} = \begin{bmatrix} 0 & 1 & 1 & 0 & 1 & 0 \\ 1 & 0 & 1 & 0 & 0 & 1 \\ 0 & 1 & 0 & 1 & 0 & 1 \\ 1 & 0 & 0 & 1 & 1 & 0 \end{bmatrix}. \tag{5}$$

Generally, message passing algorithm (MPA) or improved version of MPA is used for SCMA decoding. The conventional MPA detection involves three sequential steps: 1) Initialize the conditional probability. 2) Iterative message passing between RNs and UNs. 3) Calculate Log-Likelihood-Ratio (LLR). After a number of iterations, the final LLR values can be used for the likelihood of the codeword at each user.

C. UAV Energy Consumption Model and Channel Model

Thanks to UAV-BS's flexible and mobile nature, it can keep up LoS connection with most devices. However, the blockages may affect the UAV-to-ground device links, especially in urban scenarios. Thus, a probabilistic LoS channel model is considered, which includes both the LoS and NLoS components, dependent on the UAV deployment environment [4], [23]. The probability of the LoS link between the jth user and UAV-BS at time slot m is given by:

$$Pr_j^{LoS}[m] = \frac{1}{1 + ae^{-b(\theta_j[m]-a)}}, \tag{6}$$

where a and b are the constants depending on the carrier frequency f_c and environmental conditions, respectively [39]. θ_j denotes the elevation angle in degrees from the jth user to the UAV-BS. It is given as $\theta_j[m] = (\frac{180}{\pi})\tan^{-1}(\frac{z[m]}{r_j[m]})$, where $r_j[m]$ denotes the 2D distance from UAV-BS at time slot m to jth user denoted as $r_j[m] = \sqrt{(x[m]-x_j)^2 + (y[m]-y_j)^2}$. Correspondingly, the NLoS probability is $Pr^j_{NLoS}[m] = 1 - Pr^j_{LoS}[m]$. Next, the path loss is computed as [40]

$$L_j^{LoS}[m] = \left(\frac{4\pi f_c d_j[m]}{c}\right)^{\alpha} \eta_{LoS}, \tag{7}$$

$$L_j^{NLoS}[m] = \left(\frac{4\pi f_c d_j[m]}{c}\right)^{\alpha} \eta_{NLoS}, \tag{8}$$

where c is the speed of light, and α is the path loss exponent. η_{LoS} and η_{NLoS} are the path loss coefficients for LoS and NLoS paths, respectively. The average channel gain between the jth user and UAV at the mth time-slot is

$$G_j[m] = \frac{1}{Pr_j^{LoS} L_j^{LoS} + Pr_j^{NLoS} L_j^{NLoS}}.$$

For rotary-wing UAVs, the considered propulsion power consumption model is dependent on velocity V [23] as follows:

$$P(V) = P_o\left(1 + \frac{3V^2}{U_{tip}^2}\right) + P_i\left(\sqrt{1 + \frac{V^4}{4v_o^4}} - \frac{V^2}{2v_o^2}\right)^{1/2} + \frac{1}{2} d_o \rho s A_r V^3, \tag{9}$$

where P_o represents the blade profile power, P_i represents the induced power, U_{tip} represents rotor blade's tip speed, v_0 represents the rotor induced velocity, d_o represents the fuselage drag ratio, s represents the rotor solidity, ρ represents the air density and A_r represents the rotor disc area. During the mth slot, the UAV speed is given as $V[m] = \frac{d'[m]}{\tau[m]}$, where $d'[m] = \|\mathbf{q}[m+1] - \mathbf{q}[m]\|$. Subsequently, the energy expended by the UAV in the mth slot is expressed as $E[m] = \tau[m]P(V[m])$. Consequently, the UAV trajectory should follow the total energy constraint, denoted as $\sum_{m=1}^{M} E[m] \leq E_{max}$.

D. Problem Formulation

The overall objective of this paper is to maximize the total system sum-rate, both during UAV flight and when the UAV is in a stationary hovering state. Thus, with this objective, we have formulated two problems:

- Utilizing user locations as input, we aim to optimize the three-dimensional (3D) deployment position and trajectory of the UAV, spanning from the initial to the final deployment location. This optimization seeks to maximize the sum-rate while adhering to UAV energy constraints and ensuring a minimum rate at the deployment location. During UAV flying time, the subchannel assignment is assumed to be static and power is uniformly distributed among the users on all active subchannels.
- Upon the UAV's arrival at the deployment location, we proceed to optimize the assignment of multiple subchannels and the allocation of power across all active subchannels. This optimization aims to maximize the sum-rate within the SCMA-aided UAV system, while adhering to constraints imposed by the SCMA FGM, power budget, and the minimum user rate requirement.

In this article, our primary focus lies on subchannel assignment and power allocation when the UAV is in a hovering state. This emphasis is driven by the assumption that the UAV will spend a significant portion of its time and energy while hovering, as compared to flying.

Next, we discuss the optimization problems mathematically. In *Problem 1*, the goal is to obtain the UAV 3D deployment location, $\mathbf{L} = [x^*, y^*, z^*]$ and UAV trajectory

$\mathbf{Q} = \{\mathbf{q}_m, \forall\ m = 1, \cdots, M\}$ from the initial location (x_0, y_0, H_{min}) to the final location $\mathbf{L}$ to maximize the system sum-rate under the energy budget. *Problem 1* is mathematically expressed as

$$\mathcal{P}(1): \max_{\mathbf{L},M,\mathbf{Q}} \sum_{m=1}^{M}\sum_{k=1}^{K}\sum_{j=1}^{J} \log_2(1+\gamma_{k,j}^{m}) \quad (10a)$$

$$\text{s.t.} \quad -r \le x^*, y^* \le r, H_{\min} \le z^* \le H_{\max}, \quad (10b)$$

$$\sum_{k=1}^{K} \log_2(1+\gamma_{k,j}^{\mathbf{L}}) \ge \mathrm{R}_{\min}, \quad (10c)$$

$$z[m] \ge H_{min},\ \forall\ m \in [1, M], \quad (10d)$$

$$\|\mathbf{q}[m+1] - \mathbf{q}[m]\|^2 \le d_{max}^2, \quad (10e)$$

$$\mathbf{q}[M] = \mathbf{L}, \quad (10f)$$

$$M \le M_a, \quad (10g)$$

where r denotes the radius of the circular area, $H_{\min}$ and $H_{\max}$ is the minimum and maximum height allowed for the UAV, $\gamma_{k,j}^{\mathbf{L}}$ denotes the SINR of user j at RE k at the UAV deployment location $\mathbf{L}$, $\mathrm{R}_{\min}$ is the minimum required rate of each user and M_a denotes the maximum number of available time slots for UAV to reach $\mathbf{L}$ under the available energy budget. Constraint (10c) ensures that each user is provided the minimum rate $R_{\min}$ at the deployment location. Constraints (10e) imply that the maximum distance a UAV covers in a slot is d_{max}. The allowed $H_{\max}$ according to federal aviation authority (FAA) regulations is 122 m [41].

In *Problem 2*, the FGM and power allocation matrix are optimized to maximize the sum-rate, subject to the constraints of UAV, SCMA, and required minimum data rate to the end users. Let $\mathbf{P} = (p_{k,j})_{K\times J}$ denotes the power allocation matrix, where $p_{k,j}$ denotes the power allocated to user j on RE k. Also, it is essential to optimize the FGM of SCMA for different channel conditions. *Problem 2* can be mathematically expressed as:

$$\mathcal{P}(2): \max_{\mathbf{F},\mathbf{P}} R_S = \sum_{k=1}^{K}\sum_{j=1}^{J} \log_2(1+\gamma_{k,j}) \quad (11a)$$

$$\text{s.t.} \quad f_{k,j} \in \{0,1\},\ \forall\ 1 \le k \le K, 1 \le j \le J, \quad (11b)$$

$$\mathbf{F}_j \ne \mathbf{F}_{j'}, \quad \forall\ j \ne j' \in J, \quad (11c)$$

$$\sum_{j=1}^{J} f_{k,j} \le d_f, \quad \forall\ k \in K, \quad (11d)$$

$$\sum_{k=1}^{K} f_{k,j} \le d_v, \quad \forall\ j \in J, \quad (11e)$$

$$p_{k,j} \ge 0, \quad \forall\ 1 \le k \le K, 1 \le j \le J, \quad (11f)$$

$$\sum_{k=1}^{K}\sum_{j=1}^{J} f_{k,j}p_{k,j} \le \mathrm{P}_{\text{tot}}, \quad (11g)$$

$$\sum_{k=1}^{K} \log_2(1+\gamma_{k,j}) \ge \mathrm{R}_{\min}, \quad (11h)$$

where P_{tot} represents the total transmit power allocated for communication at UAV. Constraint (11c) represents that FGM should not have any two columns same. Constraint (11d) denotes the limit of the maximum number of users whose data are superimposed on each RE, and constraint (11e) denotes that a user is communicating over maximum d_v number of REs. Constraint (11g) ensures that the total power allocated to all the user on active subchannels is less than or equal to P_{tot}. Constraint (11h) ensures that each user is provided the minimum rate $R_{\min}$. In SCMA, CB of user j has non-zero values only at active subchannels, which is denoted by indices where FGM $\mathbf{F}$ has ones at the jth column, i.e. $f_{k,j} = 1$. Thus, constraint (11e) also denotes that CB of user j has non-zero values over maximum d_v number of REs.

Both of the optimization problems discussed in $\mathcal{P}(1)$ and $\mathcal{P}(2)$ have non-concave objective in nature, making it difficult to compute the global optimal solution [42]. Also, Problem $(\mathcal{P}2)$ is a non-convex nonlinear integer programming problem that is intractable.

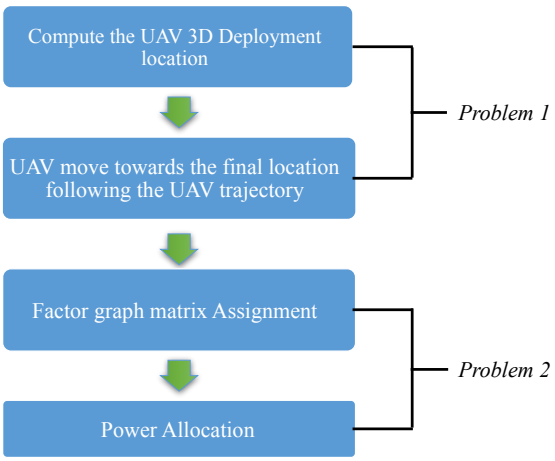

Fig. 3. Proposed solution outline.

IV. Proposed Solution

In this section, we discuss the proposed solution as outlined in Fig. 3. We first solve *Problem 1*, i.e., UAV 3D deployment and trajectory. From this, we get the information of where UAV should be deployed and what trajectory would it take. Then we solve *Problem 2* to allocate frequency subcarrier and power to each user at the UAV to maximize the system sum-rate considering the UAV and SCMA constraints.

A. Problem 1 Solution

To solve *Problem 1*, we divide it into two sub-problems and then solve them separately. First, the 3D UAV deployment location is decided. Then, the trajectory is designed between the given initial location and the final deployment location.

Algorithm 1: Proposed algorithm for computing the UAV 3D deployment location

Input: Given the location and CSI of users.
Output: Maximum sum-rate and UAV 3D deployment location.
Initialize: The initial 2D location of UAV is the geometric center of the users keeping the UAV height at H_{min}.
while $R_S^{n+1} - R_S^n \leq \epsilon$ **do**
  Calculate Δ_x^n and Δ_y^n.
  Calculate the step size using (16).
  Update the x and y coordinate of the UAV using (14) and (15).
end while
return x^*, y^*
for $zl = H_{min} : H_{max}$ **do**
  Calculate sum-rate R_S^{zl} at UAV location $[x^*, y^*, zl]$.
  Calculate the minimum rate of all users MR_{jmin}^{zl} at UAV location $[x^*, y^*, zl]$.
end for
$[indz]$ = find$(MR_{jmin}^{zl} \geq R_{min})$.
$[R_S^*, x^*, y^*, z^*] = max(R_S[x^*, y^*, indz])$.

1) UAV Deployment Location: The UAV deployment problem can be reformulated as

$$\mathcal{P}(\text{A1}): \quad \max_{\mathbf{L}} f_{\text{A1}}(\mathbf{L}) = \sum_{k=1}^{K}\sum_{j=1}^{J} \log_2(1+\gamma_{k,j}) \tag{12a}$$

$$\text{s.t.} \quad (10\text{b}), (10\text{c}). \tag{12b}$$

To solve the problem (12), we divide it into two parts: (1) find the UAV 2D deployment location, (2) find UAV-BS altitude. Firstly, the UAV 2D deployment is mathematically expressed as:

$$\mathcal{P}(\text{SP}_1): \quad \max_{x^*, y^*} \sum_{k=1}^{K}\sum_{j=1}^{J} \log_2(1+\gamma_{k,j}) \tag{13a}$$

$$\text{s.t.} \quad -r \leq x^*, y^* \leq r. \tag{13b}$$

Using the gradient ascent method, we aim to compute the UAV 2D deployment location as shown in Algorithm 1. In this, the UAV x and y coordinates are updated iteratively as follows:

$$x_{n+1} = x_n + \mu_x^n \Delta_x^n, \tag{14}$$

$$y_{n+1} = y_n + \mu_y^n \Delta_y^n, \tag{15}$$

where x_n denotes the UAV x coordinate at the nth iteration, $\mu_x^n > 0$ and $\mu_y^n > 0$ denotes the step-size with respect to UAV x and y coordinate at the nth iteration. Δ_x^n and Δ_y^n denote the derivative of the sum-rate with respect to UAV x and y coordinate at nth iteration. Now, to enhance the convergence rate of the proposed algorithm, the step size is normalized by the norm of the gradient as [43], [44]

$$\mu_x^n = \frac{L}{\|\Delta_x^n\|}, \ \mu_y^n = \frac{L}{\|\Delta_y^n\|}, \tag{16}$$

where, $L = \frac{a}{n^b}$ and we set positive constants $a = 2$ and $b = 0.6$, which may vary depending on the simulation setup.

The initial 2D UAV location is assumed to be the centroid location of all users, keeping the UAV height at H_{min}. We say that the UAV 2D location has converged when the fractional increase in the sum-rate is less than 1%. Next, we change the z coordinate from H_{min} to H_{max}, and choose the UAV 3D location, which gives maximum sum-rate under minimum rate constraint.

2) Designing UAV 3D Trajectory: Let $\mathbf{q}[0]$ denotes the initial location with minimum height, i.e., (x_0, y_0, H_{min}). Let $R_{sm}[m]$ be the sum-rate at the mth time slot, and is given as $R_{sm}[m] = \sum_{k=1}^{K}\sum_{j=1}^{J} \log_2(1+\gamma_{k,j}^m)$. Then, the UAV 3D trajectory sub-problem is reformulated as

$$\mathcal{P}(\text{A2}): \quad \max_{M, \mathbf{Q}} f_{\text{A2}}(M, \mathbf{Q}) = \sum_{m=1}^{M} R_{sm}[m] \tag{17a}$$

$$\text{s.t.} \quad (10\text{d}), (10\text{e}), (10\text{f}), (10\text{g}). \tag{17b}$$

A gradient ascent based scheme is proposed to solve $\mathcal{P}(A2)$ that computes the best UAV position in each time slot. This scheme is done sequentially for every time slot till the UAV gets to the final deployment location. Since, a UAV can cover a span of τV in every time slot, the search area for the next UAV location in mth time slot is a sphere centered at $\mathbf{q}[m-1]$ and of radius τV. As the search space is a sphere, we move to the spherical coordinate system for ease in mathematical analysis. The UAV location at the time-slot m is dependent on the azimuth angle Φ and polar angle θ with respect to origin. Then, the UAV location in terms of spherical coordinates are given as:

$$\begin{aligned} x[m] &= \tau V \cos\theta[m] \sin\Phi[m] + x[m-1], \\ y[m] &= \tau V \sin\theta[m] \sin\Phi[m] + y[m-1], \\ \text{and } z[m] &= \tau V \cos\Phi[m] + z[m-1]. \end{aligned} \tag{18}$$

Now, the sum-rate at the mth time slot becomes a function of the polar and azimuth angles. If the UAV moves sequentially in each time slot in this manner, it is not very sure that the UAV will be able to reach the final deployment location under the available energy budget. Thus, the objective is to maximize the system sum-rate and obtain the respective UAV location for a certain number of time slots (say β). After that, UAV moves as a straight-flight from the current position to deployment location $\mathbf{L}$. The parameter β is dependent on number of time-slots in which UAV can arrive location $\mathbf{L}$ under given energy budget.

In Algorithm 2, gradient ascent method works as a primary component to compute the optimal UAV location in each time slot. In time slot m, firstly a line segment is drawn between $\mathbf{q}(m-1)$ and $\mathbf{L}$. Next, the intersection point (X_m^{ini}) of the line segment and the searching sphere is calculated. X_m^{ini} is considered as an initial UAV location with $\Phi(0)[m]$ and $\theta(0)[m]$. Next, the positive gradient of the sum-rate with respect to θ and Φ are calculated. The gradient provides the direction, and the step size decides how far UAV moves in that direction. The step size with respect to θ, i.e., $\kappa(\theta^i))$ and with respect to Φ, i.e., $(\kappa(\Phi^i))$ at iteration i is normalized by the norm of the gradient. The steepest ascent is applied iteratively until $\Delta R_{sm}(\theta[m], \Phi[m]) \leq \epsilon$, where ϵ is the tolerance level, and thus the final UAV location of mth time slot is obtained at $\theta^*[m], \Phi^*[m]$. Using (18), UAV location is given in Cartesian coordinate system as

Algorithm 2: Proposed UAV 3D Trajectory Scheme

Inputs: $\mathbf{q}[0], \mathbf{L}, E_{max}, M_a, (x_j, y_j)\ \forall j = 1, \cdots, J$.
Output: M^* and $\{\mathbf{q}^*[m]\}_{m=1}^{M^*}$.
Initialize: $\beta = M_a$.
for $m = 1 : \beta$ **do**
  Draw a sphere at $\mathbf{q}[m-1]$ of radius τV, and draw a line segment between $\mathbf{L}$ and $\mathbf{q}[m-1]$. The intersection point of the line segment and sphere is denoted as X_m^{ini}.
  Compute $\theta_0[m], \Phi_0[m]$ at X_m^{ini}.
  Set $i = 1$.
  while $\Delta R_{sm}(\theta[m], \Phi[m]) \geq \epsilon$ **do**
    $\theta^{i+1} = \theta^i + \kappa(\theta^i)\Delta R_{sm}(\theta^i[m])$
    $\Phi^{i+1} = \Phi^i + \kappa(\Phi^i)\Delta R_{sm}(\Phi^i[m])$
    $i = i + 1$.
  end while
end for
if $(x[M_a], y[M_a], z[M_a]) = \mathbf{L}$ **then**
  The $\{\mathbf{q}^*[m]\}_{m=1}^{M^*}$ is the final UAV trajectory.
else
  while $M < M_a$ **do**
    Decrement β by one. Take a straight flight from $\mathbf{X}_0 = (x^*[\beta-1], y^*[\beta-1], z^*[\beta-1])$ to $\mathbf{L}$. Then, $M^* = \lceil \frac{\|\mathbf{X}_0 - \mathbf{L}\|}{\tau V} \rceil + (\beta - 1)$. The final trajectory is $(x^*[m], y^*[m], z^*[m])_{m=\beta}^{M^*}$
  end while
end if

Algorithm 3: The proposed $\mathbf{F}$ assignment algorithm

Inputs:
$\mathbf{H}_{K\times J}$: Channel gain matrix, d_f, d_v.
Output:
$\mathbf{F}_{K\times J}$
Initialize:
Initialize $(\mathbf{F}_{\text{ini}})_{K\times J}$ as an all-ones matrix, and $\mathbf{F}_{K\times J}$ as a zero matrix.
Calculate the SINR matrix $\mathbf{S}_{K\times J} = (\gamma_{k,j})_{K\times J}$.
Calculate the average RMS value, $\mathbf{r}$ from $\mathbf{S}$ with respect to each user.
Sort the RMS values $\mathbf{r}$ in descending order.
for $j = 1 : J$ **do**
  if $\sum_{j=1}^{J} \mathbf{F}_{k,j} \leq d_f,\ \forall 1 \leq k \leq K$ or $\mathbf{F}_j \neq \mathbf{F}_{j'},\ \forall j \neq j' \in J$ **then**
    Find the highest d_v number of values from the $\mathbf{r}(j)$ column of $\mathbf{S}$, and store the corresponding indices in $\mathbf{c}_j$.
    For the indices stored in $\mathbf{c}_j$, set their corresponding indices equal to one in $\mathbf{F}_j$ column.
    For the $\mathbf{r}(j)$ column in $\mathbf{S}$, set the d_v largest value equal to zero.
  else
    Follow the similar steps 6-8 for the indices of the next d_v highest values.
  end if
end for

$(x^*[m], y^*[m], z^*[m])$. Thus, for initial β number of slots, the UAV trajectory is obtained using gradient ascent method.

Algorithm 2 is used to calculate the suitable value of β and the respective UAV 3D trajectory. In Algorithm 2, the β is initialized as equal to M_a. Then, the UAV trajectory is calculated using the gradient ascent method for $\beta = M_a$ slots. If UAV reaches the final deployment location under $\beta = M_a$ number of slots, then the algorithm stops and we obtain the final sub-optimal UAV trajectory. If not, β is decreased by 1, and the UAV trajectory for this new β uses the same locations as obtained previously (with $\beta = M_a$). Then, for $m \geq \beta$ time slots, it takes a straight-flight to get to $\mathbf{L}$. Thus, for new β, we get the value of M^* required to get to location $\mathbf{L}$. We follow similar steps for each decremented β, until UAV reaches location $\mathbf{L}$ under the given energy budget.

B. Problem 2 Solution

In the previous sub-section, we have obtained the deployment location and designed the UAV trajectory for the given energy budget. Now, as UAV has reached near the users, we start allocating the resources, i.e., frequency and power to each user judiciously.

1) Designing $\boldsymbol{F}$ for a given $\boldsymbol{P}$: With known $\mathbf{P}$, (11) can be reformed as:

$$\mathcal{P}(\text{A3}): \quad \max_{\mathbf{F}} f_{\text{A3}}(\mathbf{F}) = \sum_{k=1}^{K}\sum_{j=1}^{J} \log_2(1+\gamma_{k,j}) \tag{19a}$$

$$\text{s.t.} \quad (11\text{b}), (11\text{c}), (11\text{d}), (11\text{e}). \tag{19b}$$

To solve the problem $\mathcal{P}(\text{A3})$, $\mathbf{F}$ is computed using the proposed algorithm in **Algorithm 3**. This algorithm utilize the CSI available at the UAV-BS. In **Algorithm 3**, we initially consider a $\mathbf{F}_{\text{ini}}$ as an all-ones matrix of size $K \times J$. Then, the SINR matrix $\mathbf{S}_{K\times J} = (\gamma_{k,j})_{K\times J}$ is calculated, where $\gamma_{k,j}$ is as shown in (2). Next, the root mean square (RMS) of $\mathbf{S}$ is calculated with respect to the users and then sorted in the descending order. The RE allotment starts with the user having the highest RMS value. For this user, d_v REs with the highest SINR are chosen and these REs are assigned to the corresponding user. A similar procedure is repeated for all the users sequentially with decreasing RMS values. With the allocation of REs to each user, fulfilling the constraints in (11d), (11e), (11c) becomes more difficult as the users increase. In that case, we keep choosing the next d_v number of RES corresponding to next highest SINR values until all the constraints are fulfilled. Thus, this algorithm basically gives the priority to the subcarrier on which user is getting good SINR, considering the SCMA CB constraints.

2) Power Allocation : For the given FGM $\mathbf{F}$, the sum-rate optimization problem in (11) becomes:

$$\mathcal{P}(\text{A4}): \quad \max_{\mathbf{P}} f_{\text{A4}}(\mathbf{P}) = \sum_{k=1}^{K}\sum_{j=1}^{J} \log_2(1+\gamma_{k,j}) \tag{20a}$$

$$\text{s.t.} \quad (11\text{g}), (11\text{h}), (11\text{f}). \tag{20b}$$

Here, subproblem (20) is a non-convex problem, and the complexity of finding the optimal solution is prohibitive. Thus, we use Lagrange dual decomposition method to find a near-optimal solution. The basic idea here is that we augment the objective function with a weighted sum of the constraint functions. The Lagrangian of (20) is given as

$$L(\{\mathbf{P}\}, \boldsymbol{\lambda}, \zeta) = \sum_{j=1}^{J}\left[(1+\lambda_j)\sum_{k=1}^{K}\log_2(1+\gamma_{k,j}) - \lambda_j \text{R}_{\min}\right] + \zeta\left(\text{P}_{\text{tot}} - \sum_{k=1}^{K}\sum_{j=1}^{J} p_{k,j}\right), \tag{21}$$

where $\boldsymbol{\lambda} = \{\lambda_1, \cdots, \lambda_J\}$, and λ_j and ζ are the Lagrange multipliers associated with jth user. The dual objective function is given as $\mathcal{G}(\boldsymbol{\lambda}, \zeta) = \max_{\{\mathbf{P}\}} L(\{\mathbf{P}\}, \boldsymbol{\lambda}, \zeta)$, and thus the dual problem becomes

$$\min_{\boldsymbol{\lambda}, \zeta} \mathcal{G}(\boldsymbol{\lambda}, \zeta) \tag{22a}$$

$$\text{s.t.} \quad \boldsymbol{\lambda}, \zeta \succcurlyeq 0. \tag{22b}$$

The KKT conditions are applied [45] to (22). Next, the Lagrangian in (21) is differentiated with the variable $p_{k,j}$, and then equated to zero. Thus, we obtain

$$\frac{(1+\lambda_j)\ g_{k,j}}{\ln(2).(1+\sum_{i \in S_k} p_{k,i}\ g_{k,i})} \approx \zeta, \tag{23}$$

where $g_{k,j}$ is the normalized channel gain with respect to user j at RE k. The approximation arises due to the inter-user interference which can be mitigated by the proper design of CB. Thus,

$$\hat{p}_{k,j} = \left[\frac{(1+\lambda_j)}{\zeta\ \ln(2)} - \frac{1}{\frac{g_{k,j}}{1+\sum\limits_{\substack{i \in S_k \\ i \neq j}} p_{k,i}\ g_{k,i}}} \right]^+, \tag{24}$$

where $[x]^+$ denotes the max(0, x) operation. The variable $p_{k,j}$ is substituted into function L given in (21). Now, L becomes a function of Lagrange multipliers, and the dual problem in (22) can be solved with commercially available optimization solvers. After solving this, we get the optimal value of Lagrange multipliers. Lastly, $p_{k,j}$ can be calculated by substituting the obtained value of Lagrangian multipliers in (24). For this non-convex optimization problem (20), there exists a duality gap, but it tends to zero as the number of subcarriers increase [46].

C. Complexity

The *Problem 1* is divided into two subproblems as: solving the optimization with respect to the 3D UAV deployment location and optimizing the UAV trajectory. The complexity of **Algorithm 1** for UAV deployment is primarily dependent on the complexity of gradient ascent. Let the complexity of computing the derivative for UAV 2D deployment location be $O(a_1)$ and the number of required iterations be N_{xy}. Thus, the total complexity to compute the sub-optimal solution of computing $\mathbf{L}$ is $O(N_{xy}a_1 + Z_{range})$, where Z_{range} is the altitude range for checking the UAV deployment location. In **Algorithm 2**, the gradient ascent algorithm is called for M_a number of time slots. Thus, the total complexity of **Algorithm 2** is $O(M_a a_2 N_{tp})$, where a_2 denotes the computation cost for calculating the gradient of the sum-rate with respect to θ and Φ in each slot, and N_{tp} denotes the number of iterations required for updating the azimuth and polar angle.

In *Problem 2*, FGM $\mathbf{F}$ and the power allocation matrix $\mathbf{P}$ are optimized. The complexity of **Algorithm 3** for FGM assignment is contingent upon both the number of users and the prevailing channel conditions. Within **Algorithm 3**, d_v REs exhibiting the most favorable channel conditions are selected for a single user, and these REs are indexed with the value one for the CB associated with that user. Let a_3 denote the complexity associated with selecting d_v REs for each user with the most favorable channel conditions. Consequently, whenever the indices coincide with those of other users, the complexity experiences an increment of $O(a_3)$. Hence, the complexity of **Algorithm 3** is a constant value multiplied by the number of users, and it is proportional to $O(J)$. Moreover, the complexity of the power allocation algorithm is contingent on solving the dual problem. Thus, the complexity associated with solving the dual problem is $O(I_f(Jd_v))$, where I_f represents the number of iterations needed to compute the dual variables. So, the total complexity for solving *Problem 2* is $O(J + (I_f(Jd_v)))$.

V. Results and Discussion

In this section, we evaluate the performance of the proposed algorithms along with benchmark schemes. The simulation setup consists of a UAV working as an aerial BS and serves J ground users. The users are randomly distributed in a circular field of radius 200 m, centered at (250 m, 250 m). The UAV minimum height H_{min} is 20 m. The tolerance value is $\epsilon = 0.01$. The simulation parameters are : $P_i = 88.63$ W, $P_o = 79.86$ W, $v_o = 4.03$ m/s, $U_{tip} = 120$, $d_o = 0.6, s = 0.05$, ρ = 1.225, and $A_r = 0.503$, $a = 11.95$, $b = 0.136$, $\mathrm{P_{tot}} = 30$ dBm, $\alpha = 2.5$, $\tau = 1$ s, $(x_0, y_0, 0) = (100, 100, 0)$ m, $\eta_{LoS} = 3$ dB and $\eta_{NLoS} = 23$ dB. We assume that the small-scale fading is in a Rayleigh distribution with the unit mean [47].

In the baseline SCMA scheme, UAV is assumed to be at the geometric center of all the users, with static $\mathbf{F}$ and uniform power allocation, respectively. We compare the sum-rate performance of baseline SCMA scheme with a standard NOMA scheme, called PD-NOMA, and an OMA scheme. In PD-NOMA, users are ordered based on their channel strength, and the power is allocated in such a manner that more power is allocated to the weak user under the given power budget [8]. We have implemented the time-division multiple-access (TDMA) scheme in the OMA scheme. In both schemes, the users are assumed to communicate over a single subcarrier. The results are analysed based on the optimization variables, i.e., where the UAV should be deployed, how the resources are managed while serving the users, and how the UAV reaches the desired location.

A. Performance Analysis for 4×6 and 5×10 SCMA Block

Fig. 4 shows the sum-rate performance with respect to the UAV's total transmit power, specifically for a scenario where six users are served across four subchannels. Initially, we present the performance of OMA, PD-NOMA, and the baseline SCMA scheme. Subsequently, we gradually introduce the proposed enhancements, encompassing the proposed UAV 3D deployment location, FGM, and power allocation schemes, one after the other. Firstly, we employ **Algorithm 1**

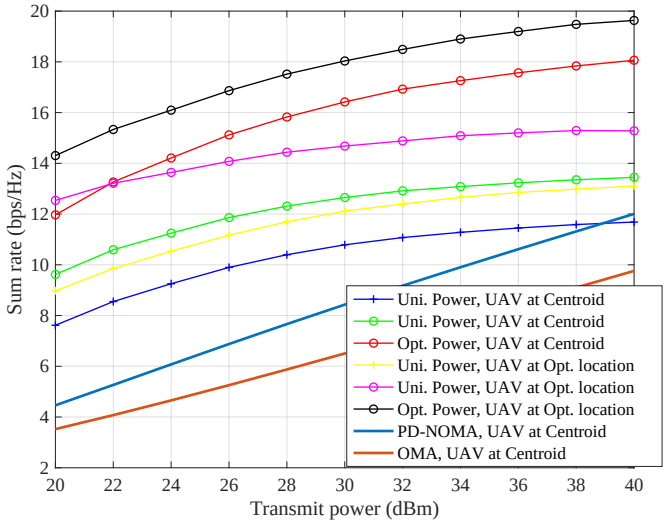

Fig. 4. Sum-rate versus UAV transmit power for $K = 4$ and $J = 6$, where 'Uni.' represents uniform, 'Opt.' represents the optimized, '+' represents the fixed **F** and 'o' represents proposed **F**.

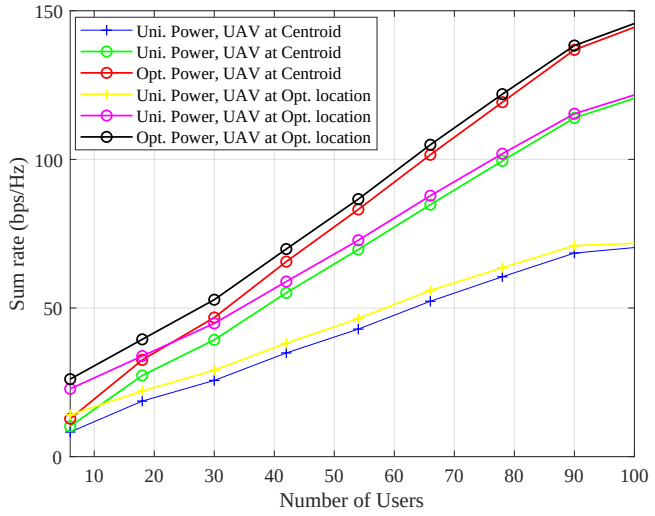

Fig. 5. Sum-rate versus number of users for UAV-SCMA system, where 'Uni.' represents uniform, 'Opt.' represents the optimized, '+' represents the fixed **F** and 'o' represents the proposed **F**.

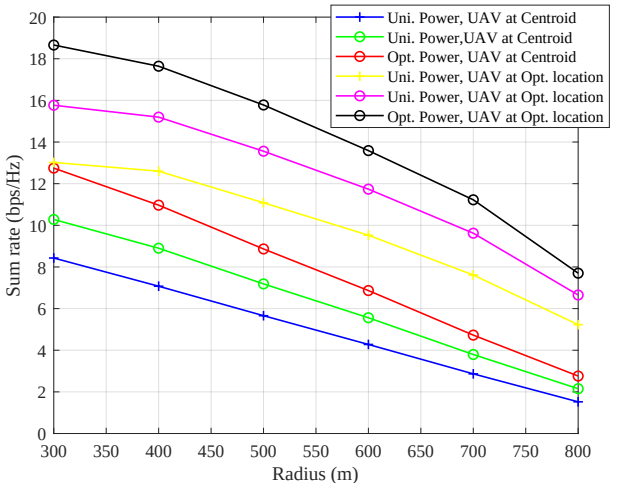

Fig. 6. Sum-rate versus radius of circular field for 4×6 SCMA block, where 'Uni.' represents uniform, 'Opt.' represents the optimized, '+' represents the fixed **F** and 'o' represents the proposed **F**.

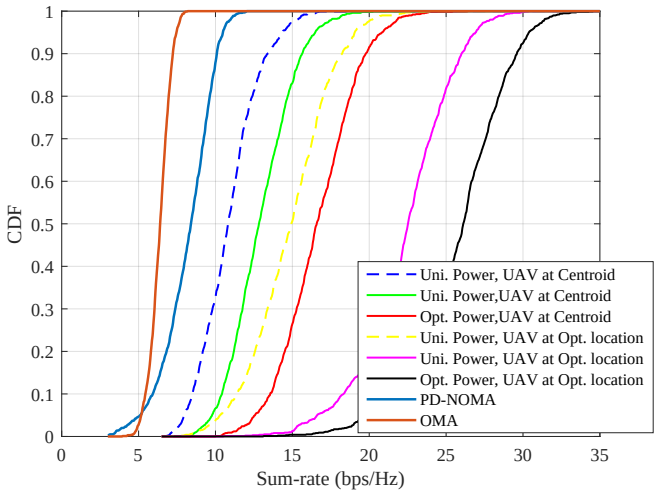

Fig. 7. CDF curves for 4×6 SCMA block at UAV transmit power of 30 dBm, where 'Uni.' denotes uniform, 'Opt.' denotes the optimized, dashed line represents static **F** as shown in (5), and solid line denotes **F** generated from Algorithm 3.

to compute the UAV 3D deployment based on the location of ground users. With optimized UAV deployment, the system sum-rate gets improved as compared to the performance for UAV located at the geometric center of the users. Then, we optimize the FGM using the **Algorithm 3**, and uniform power is considered. With the assignment of **F**, the association between the user and REs is decided, and then power allocation is done to all users for every associated RE with Lagrange dual decomposition method. It is evident that with the proposed algorithms, the sum-rate performance notably improves as the transmit power increases.

Fig. 5 shows the sum-rate performance with respect to the number of users. It is to be noted that initially, the improvement in sum-rate at the optimal UAV location is more than the UAV at the geometric center, but as J increases, the impact of UAV deployment is relatively smaller. However, it is noted that FGM assignment and power allocation shows an improved sum rate as the number of users increase. This means that it is more crucial to carefully allocate REs and power as the number of users increase.

Fig. 6 shows the sum-rate performance with increasing radius r of the circular area for $J = 6$ users. As the radius increases, there is a corresponding rise in path loss, resulting in a decrease in the sum-rate for all the schemes. It is worth highlighting that through the optimization of UAV deployment, multiple subchannel assignment, and power allocation, there is a noteworthy improvement in the sum-rate performance compared to the baseline SCMA scheme, even as the radius increases. Fig. 7 illustrates the cumulative distribution function (CDF) of the system sum-rate concerning OMA, PD-NOMA, and the baseline SCMA schemes. Subsequently,

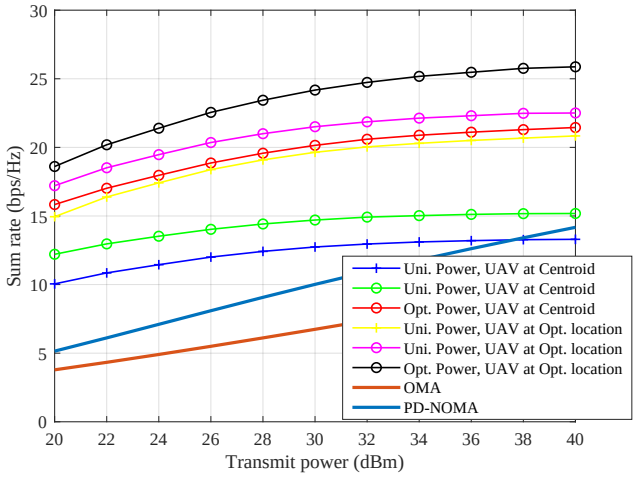

Fig. 8. Sum-rate versus UAV transmit power for $K = 5$ and $J = 10$, where 'Uni.' denotes uniform, 'Opt.' denotes the optimized, '+' denotes the fixed $\mathbf{F}$ and 'o' denotes the proposed $\mathbf{F}$

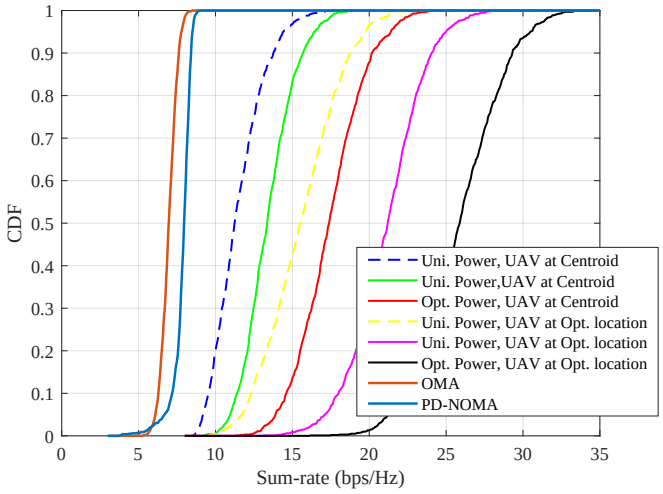

Fig. 9. CDF curves for 5×10 SCMA block at transmit power of 30 dBm, where 'Uni.' denotes uniform, 'Opt.' denotes the optimized, dashed line represents static $\mathbf{F}$ as shown in (25), and solid line denotes $\mathbf{F}$ generated from Algorithm 3.

it demonstrates the influence of optimizing UAV deployment, subchannel assignment, and power allocation. It is to be noted that the the gains of the proposed methods remain consistently stable, surpassing the performance of benchmark schemes, and the curves are consistent with their counterparts in Fig. 4.

Next, we consider 5×10 SCMA block in which ten users are served using five subcarriers, i.e., overloading factor is equal to $J/K = 2$. An example of the $\mathbf{F}_{5\times10}$ is shown below [48]

$$\mathbf{F}_{5\times10} = \begin{bmatrix} 1 & 1 & 1 & 1 & 0 & 0 & 0 & 0 & 0 & 0 \\ 1 & 0 & 0 & 0 & 1 & 1 & 1 & 0 & 0 & 0 \\ 0 & 1 & 0 & 0 & 1 & 0 & 0 & 1 & 1 & 0 \\ 0 & 0 & 1 & 0 & 0 & 1 & 0 & 1 & 0 & 1 \\ 0 & 0 & 0 & 1 & 0 & 0 & 1 & 0 & 1 & 1 \end{bmatrix}. \quad (25)$$

Fig. 8 shows the sum-rate performance of OMA, PD-NOMA, and the proposed methods for SCMA with respect to UAV total transmit power for ten users. Here, the total transmit power has been divided among ten users; therefore, power allotted to each user is less than for $J = 6$ case, and d_f also increases to four. It is worth noting that, even though the overloading factor $\frac{J}{K}$ is increased to two, the proposed algorithms perform better, and the sum-rate improves with the increase in transmit power. Fig. 9 displays the CDF curves depicting the sum-rate of both benchmark and proposed schemes across various channel realizations. Notably, the sum-rate of the proposed methods consistently outperforms that of the benchmark schemes, demonstrating superior performance regardless of the overloading factor and specific channel realizations.

B. Sum-Rate Analysis for Proposed UAV Trajectory

Fig. 10 shows the insights of the proposed and benchmark UAV trajectories. The benchmark schemes are straight flight and fly-hover schemes [49]. In the straight flight scheme, the

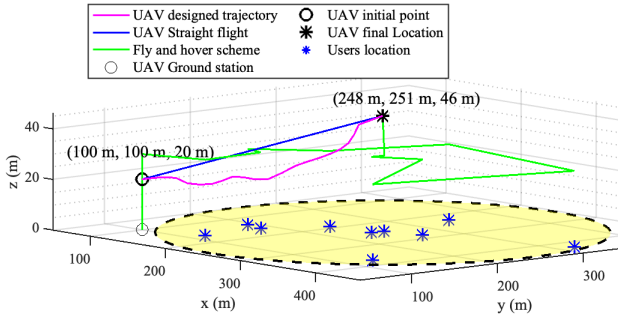

Fig. 10. Insights on 3-D UAV trajectories.

UAV follows a linear trajectory, i.e., moving along a straight-line path from the initial to the final deployment location. In the fly-hover scheme, the process involves initially calculating a sequence of hovering locations, each corresponding to the user's position at a constant height, spanning from the initial to the final deployment location. Subsequently, the UAV moves to these hovering locations before reaching the ultimate deployment destination. In the proposed method, the UAV initially moves towards the space where the sum-rate with respect to the users is higher, thus providing improved sum-rate performance than the benchmark schemes.

Fig. 11 shows the sum-rate performance averaged over number of users for the proposed UAV trajectory along with benchmark schemes for the given energy consumption. As the energy budget increases, all the schemes exhibit an enhancement in system sum-rate. However, the proposed scheme outperforms both the fly-hover scheme and straight-flight scheme, yielding the highest sum-rate improvement within the specified energy budget. Fig. 12 illustrates the CDF of the average sum-rate associated with the proposed 3D UAV trajectory for both SCMA and PD-NOMA schemes. It is to be noted that the proposed trajectory with SCMA

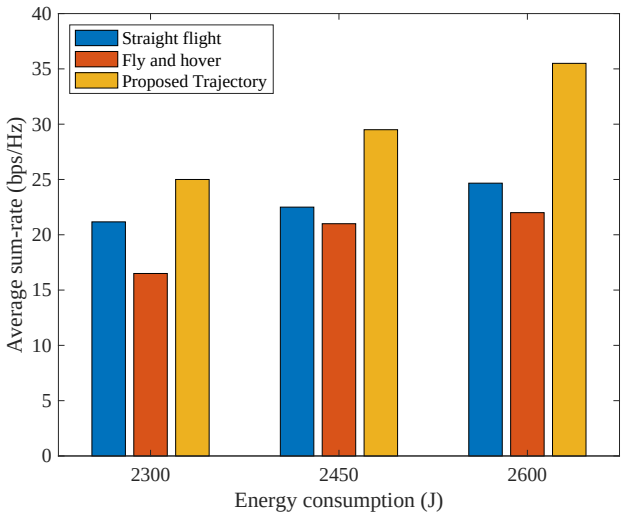

Fig. 11. Average sum-rate over the the proposed and benchmark schemes under different energy budget.

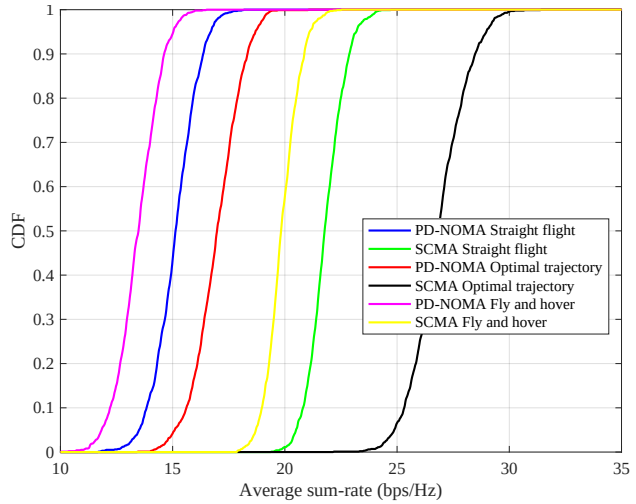

Fig. 12. CDF of average sum-rate for PD-NOMA and SCMA aided UAV trajectories.

scheme consistently outperforms the benchmark schemes as the UAV traverses towards regions with higher sum-rates.

VI. Conclusion

In this work, we have investigated an SCMA-assisted downlink UAV system, where the goal is to efficiently manage the available resources and provide improved user service. Specifically, we have formulated two optimization problems. In the first problem, we have proposed an iterative gradient ascent-based algorithm to optimize the UAV 3D deployment location and UAV trajectory in order to maximize the system sum-rate under the UAV on-board energy availability constraints. In the second problem, we optimize the allocation of spectrum resources and power, subject to the SCMA FGM and UAV power budget constraints. Such a problem has been solved by a CSI-based algorithm for spectrum allocation to each user, followed by Lagrangian dual decomposition method for power allocation. Our simulation results have demonstrated the superiority of the proposed algorithms over the benchmark schemes. Our research shows that 1) optimizing the UAV's deployment position, instead of placing it at the geometric center of the users, can enhance the system performance; 2) optimizing the UAV's trajectory, even without resource management, proves to be advantageous; 3) employing CSI-based multiple subcarrier allocation and strategic power allocation can significantly improve system performance compared to static subcarrier allocation and uniform power distribution. As a future work, we plan to explore the resource management problem in multiple UAV network, where inter-UAV interference plays a crucial role.

References

[1] B. Li, Z. Fei, and Y. Zhang, "UAV communications for 5G and beyond: Recent advances and future trends," *IEEE Internet Things J.*, vol. 6, no. 2, pp. 2241–2263, Apr. 2019, doi: 10.1109/JIOT.2018.2887086.

[2] M. Noor-A-Rahim et al., "6G for vehicle-to-everything (V2X) communications: Enabling technologies, challenges, and opportunities," *Proc. IEEE*, vol. 110, no. 6, pp. 712–734, Jun. 2022, doi: 10.1109/JPROC.2022.3173031.

[3] Y. Zeng, R. Zhang, and T. J. Lim, "Wireless communications with unmanned aerial vehicles: opportunities and challenges," *IEEE Commun. Mag.*, vol. 54, no. 5, pp. 36–42, 2016, doi: 10.1109/MCOM.2016.7470933.

[4] M. Mozaffari, W. Saad, M. Bennis, Y. Nam, and M. Debbah, "A tutorial on UAVs for wireless networks: Applications, challenges, and open problems," *IEEE Commun. Surveys Tuts.*, vol. 21, no. 3, pp. 2334–2360, 3rd Quart., 2019, doi: 10.1109/COMST.2019.2902862.

[5] Z. Ullah, F. Al-Turjman, and L. Mostarda, "Cognition in UAV-aided 5G and beyond communications: A survey," *IEEE Trans. Cognit. Commun. Netw.*, vol. 6, no. 3, pp. 872–891, Sep. 2020, doi: 10.1109/TCCN.2020.2968311.

[6] Y. Liu, Z. Qin, M. Elkashlan, Z. Ding, A. Nallanathan, and L. Hanzo, "Non-orthogonal multiple access for 5G and beyond," *Proc. IEEE*, vol. 105, no. 12, pp. 2347–2381, Dec. 2017, doi: 10.1109/JPROC.2017.2768666.

[7] L. Yu, Z. Liu, M. Wen, D. Cai, S. Dang, Y. Wang, P. Xiao, "Sparse Code Multiple Access for 6G Wireless Communication Networks: Recent Advances and Future Directions," *IEEE Commun. Stand. Mag.*, vol. 5, no. 2, pp. 92-99, June 2021, doi: 10.1109/MCOMSTD.001.2000049.

[8] S. M. R. Islam, N. Avazov, O. A. Dobre, and K.-S. Kwak, "Power domain non-orthogonal multiple access (NOMA) in 5G systems: Potentials and challenges," *IEEE Commun. Surveys Tuts.*, vol. 19, no. 2, pp. 721–742, 2nd Quart., 2017, doi: 10.1109/COMST.2016.2621116.

[9] H. Nikopour and H. Baligh,"Sparse code multiple access," in *Proc. IEEE 24th Int. Symp. Pers. Indoor Mobile Radio Commun. (PIMRC)*, London, UK, 2013, pp. 332–336, doi: 10.1109/PIMRC.2013.6666156.

[10] M. Moltafet, N. M. Yamchi, M. R. Javan, and P. Azmi, "Comparison study between PD-NOMA and SCMA," *IEEE Trans.Veh. Technol.*, vol. 67, no. 2, pp. 1830–1834, Feb. 2018, doi: 10.1109/TVT.2017.2759910.

[11] Q. Luo et al., "An error rate comparison of power domain non-orthogonal multiple access and sparse code multiple access," *IEEE Open J. Commun. Soc.*, vol. 2, pp. 500–511, 2021, doi: 10.1109/OJCOMS.2021.3064504.

[12] S. Moon, H.-S. Lee, and J.-W. Lee, "SARA: Sparse code multiple access-applied random access for IoT devices," *IEEE Internet Things J.*, vol. 5, no. 4, pp. 3160–3174, Aug. 2018, doi: 10.1109/JIOT.2018.2835828.

[13] S. Chaturvedi, Z. Liu, V. A. Bohara, A. Srivastava and P. Xiao, "A Tutorial on Decoding Techniques of Sparse Code Multiple Access," *IEEE Access*, vol. 10, pp. 58503-58524, 2022, doi: 10.1109/ACCESS.2022.3178127.

[14] K. Deka, A. Thomas and S. Sharma, "OTFS-SCMA: A Code-Domain NOMA Approach for Orthogonal Time Frequency Space Modulation," in *IEEE Trans. Commun.*, vol. 69, no. 8, pp. 5043-5058, Aug. 2021, doi: 10.1109/TCOMM.2021.3075237.

[15] H. Wen, W. Yuan, Z. Liu and S. Li, "OTFS-SCMA: A Downlink NOMA Scheme for Massive Connectivity in High Mobility Channels," in *IEEE Trans. Wireless Commun*, doi: 10.1109/TWC.2023.3236383.

[16] H. Wen, W. Yuan, and S. Li, "Downlink OTFS non-orthogonal multiple access receiver design based on cross-domain detection," in *Proc. IEEE Int. Conf. Commun. Workshops*, 2022, pp. 928–933, doi: 10.1109/ICCWorkshops53468.2022.9814572.

[17] W. Mei and R. Zhang, "Uplink cooperative NOMA for cellular-connected UAV," *IEEE J. Sel. Top. Signal Process.*, vol. 13, no. 3, pp. 644–656, Jun. 2019, doi: 10.1109/JSTSP.2019.2899208.

[18] N. Zhao et al., "Security enhancement for NOMA-UAV networks," *IEEE Trans. Veh. Technol.*, vol. 69, no. 4, pp. 3994–4005, Apr. 2020, doi: 10.1109/TVT.2020.2972617.

[19] J. Sun, Z. Wang, and Q. Huang, "Cyclical NOMA based UAV-enabled wireless network," *IEEE Access*, vol. 7, pp. 4248–4259, Jan. 2019, doi: 10.1109/ACCESS.2018.2888855.

[20] R. Tang, J. Cheng, and Z. Cao, "Joint placement design, admission control, and power allocation for NOMA-based UAV systems," *IEEE Wireless Commun. Lett.*, vol. 9, no. 3, pp. 385–388, Mar. 2020, doi: 10.1109/LWC.2019.2956702.

[21] J. Seo, S. Pack, and H. Jin, "Uplink NOMA random access for UAV-assisted communications," *IEEE Trans. Veh. Technol.*, vol. 68, no. 8, pp. 8289–8293, Aug. 2019, doi: 10.1109/TVT.2019.2923441.

[22] P. Qin, X. Wu, Z. Cai, X. Zhao, Y. Fu, M. Wang, and S. Geng, "Joint trajectory plan and resource allocation for UAV-enabled C-NOMA in air-ground integrated 6G heterogeneous network," *IEEE Trans. Netw. Sci. Eng*, 2023, in Press. DOI:10.1109/tnse.2023.3261278.

[23] M. F. Sohail, C.Y. Leow, and S.Won, "Non-orthogonal multiple access for unmanned aerial vehicle assisted communication," *IEEE Access*, vol. 6, pp. 22 716–22727, 2018, doi: 10.1109/ACCESS.2018.2826650.

[24] X. Liu et al., "Placement and power allocation for NOMA-UAV networks," *IEEE Wireless Commun. Lett.*, vol. 8, no. 3, pp. 965–968, Jun. 2019, doi: 10.1109/LWC.2019.2904034.

[25] F. Cui, Y. Cai, Z. Qin, M. Zhao, and G. Y. Li, "Multiple access for mobile-UAV enabled networks: Joint trajectory design and resource allocation," *IEEE Trans. Commun.*, vol. 67, no. 7, pp. 4980–4994, Jul. 2019, doi: 10.1109/TCOMM.2019.2910263.

[26] N. Zhao et al., "Joint trajectory and precoding optimization for UAV-assisted NOMA networks," *IEEE Trans. Commun.*, vol. 67, no. 5, pp. 3723–3735, May 2019, doi: 10.1109/TCOMM.2019.2895831.

[27] W. Chen, S. Zhao, R. Zhang, Y. Chen, and L. Yang, "UAV-Assisted Data Collection With Nonorthogonal Multiple Access," *IEEE Internet Things J.*, vol. 8, no. 1, pp. 501–511, Jan. 2021, doi: 10.1109/JIOT.2020.3005271.

[28] W. Wang, N. Zhao, L. Chen, X. Liu, Y. Chen, and D. Niyato, "UAV-assisted time-efficient data collection via uplink NOMA," *IEEE Trans. Commun.*, vol. 69, no. 11, pp. 7851–7863, Nov. 2021, doi: 10.1109/TCOMM.2021.3106134.

[29] R. Tang, R. Zhang, Y. Xu and J. He, "Energy-efficient Optimization Algorithm in NOMA-based UAV-assisted Data Collection Systems," *IEEE Wireless Commun. Lett.*, 2022, doi: 10.1109/LWC.2022.3219675.

[30] R. Zhong, X. Liu, Y. Liu, and Y. Chen, "Multi-agent reinforcement learning in NOMA-aided UAV networks for cellular offloading," *IEEE Trans. Wireless Commun.*, vol. 21, no. 3, pp. 1498–1512, Mar. 2022, doi: 10.1109/TWC.2021.3104633.

[31] P. Qin, Y. Fu, Y. Xie, K. Wu, X. Zhang and X. Zhao, "Multi-Agent Learning-Based Optimal Task Offloading and UAV Trajectory Planning for AGIN-Power IoT," *IEEE Trans. Commun.*, vol. 71, no. 7, pp. 4005-4017, July 2023, doi: 10.1109/TCOMM.2023.3274165.

[32] A. A. Nasir, H. D. Tuan, T. Q. Duong, and H. V. Poor, "UAV-enabled communication using NOMA," *IEEE Trans. Commun.*, vol. 67, no. 7, pp. 5126–5138, Jul. 2019, doi: 10.1109/TCOMM.2019.2906622.

[33] D. Zhai, M. Sheng, X. Wang, Y. Li, J. Song and J. Li, "Rate and Energy Maximization in SCMA Networks With Wireless Information and Power Transfer," *IEEE Commun. Lett.*, vol. 20, no. 2, pp. 360-363, Feb. 2016, doi: 10.1109/LCOMM.2015.2504439.

[34] A. Sultana, I. Woungang, A. Anpalagan, L. Zhao and L. Ferdouse, "Efficient Resource Allocation in SCMA-Enabled Device-to-Device Communication for 5G Networks," *IEEE Trans. Veh. Technol.*, vol. 69, no. 5, pp. 5343-5354, May 2020, doi: 10.1109/TVT.2020.2983569.

[35] M. Cheraghy, W. Chen, H. Tang, Q. Wu and J. Li, "Joint Rate and Fairness Improvement Based on Adaptive Weighted Graph Matrix for Uplink SCMA With Randomly Distributed Users," *IEEE Trans. Commun.*, vol. 69, no. 5, pp. 3106-3118, May 2021, doi: 10.1109/TCOMM.2021.3058529.

[36] B. Zhao, J. Liu, B. Mao and S. Li, "Optimal Resource Allocation for Random Multiple Access Oriented SCMA-V2X Networks," *IEEE Trans. Veh. Technol.*, vol. 72, no. 8, pp. 10921-10932, Aug. 2023, doi: 10.1109/TVT.2023.3262274.

[37] S. Chaturvedi, V. A. Bohara, Z. Liu and A. Srivastava, "Sum-Rate Maximization of IRS-Aided SCMA System," *IEEE Trans. Veh. Technol.*, vol. 72, no. 8, pp. 10462-10472, Aug. 2023, doi: 10.1109/TVT.2023.3260976.

[38] Z. Ding, P. Fan and H. V. Poor, "Impact of User Pairing on 5G Nonorthogonal Multiple-Access Downlink Transmissions," *IEEE Trans. Veh. Technol.*, vol. 65, no. 8, pp. 6010–6023, Aug. 2016, doi: 10.1109/TVT.2015.2480766.

[39] K. Zhu, X. Xu, and S. Han, "Energy-efficient uav trajectory planning for data collection and computation in mMTC networks," in *2018 IEEE Globecom Workshops (GC Wkshps)*, 2018, pp. 1–6, doi: 10.1109/GLOCOMW.2018.8644379.

[40] A. Al-Hourani, S. Kandeepan, and S. Lardner, "Optimal LAP altitude for maximum coverage," *IEEE Wireless Commun. Lett.*, vol. 3, no. 6, pp. 569–572, 2014, doi: 10.1109/LWC.2014.2342736.

[41] X. Mu, Y. Liu, L. Guo, J. Lin, and Z. Ding, "Energy-constrained UAV data collection systems: NOMA and OMA," *IEEE Trans. Veh. Technol.*, vol. 70, no. 7, pp. 6898–6912, Jul. 2021, doi: 10.1109/TVT.2021.3086556.

[42] J. Hartmanis, "Computers and intractability: a guide to the theory of NP-completeness," *Siam Review*, vol. 24, no. 1, p. 90, 1982.

[43] I. Goodfellow, Y. Bengio, A. Courville, and Y. Bengio, *Deep learning*, MIT press Cambridge, 2016, vol. 1, no. 2.

[44] P. Singh, A. Gupta, V. A. Bohara, and A. Srivastava, "QoS-aware reliable architecture for broadband fiber- wireless access networks," *IEEE Syst. J.*, vol. 16, no. 4, pp. 5753–5764, Dec. 2022, doi: 10.1109/JSYST.2022.3149854.

[45] S. Boyd and L. Vandenberghe, *Convex Optimization*. Cambridge, U.K.: Cambridge Univ. Press, 2004.

[46] S. Han, Y. Huang, W. Meng, C. Li, N. Xu and D. Chen, "Optimal Power Allocation for SCMA Downlink Systems Based on Maximum Capacity," *IEEE Trans. Commun.*, vol. 67, Feb. 2019, pp. 1480–89, doi: 10.1109/TCOMM.2018.2877671.

[47] L. Zhou, H. Ma, Z. Yang, S. Zhou and W. Zhang, "Unmanned Aerial Vehicle Communications: Path-Loss Modeling and Evaluation," *IEEE Veh. Technol. Mag.*, vol. 15, no. 2, pp. 121-128, June 2020, doi: 10.1109/MVT.2019.2961608.

[48] Z. Liu and L.-L. Yang, "Sparse or dense: A comparative study of code-domain NOMA systems," *IEEE Trans. Wireless Commun.*, vol. 20, no. 8, pp. 4769–4780, Aug. 2021, doi: 10.1109/TWC.2021.3062235.

[49] Y. Zeng, J. Xu, and R. Zhang, "Energy minimization for wireless communication with rotary-wing UAV," *IEEE Trans. Wireless Commun.*, vol. 18, no. 4, pp. 2329–2345, Apr. 2019, doi: 10.1109/TWC.2019.2902559.